PCCP

Accepted Manuscript

ROYAL SOCIETY OF CHEMISTRY

www.rsc.org/pccp

The magnetism tuned by charge states of defects in bulk C-doped SnO_2 materials

Ying-Bo Lu, Z. C. Ling Wei-Yan Cong, and Peng Zhang

School of Space Science and Physics, Shandong University, Weihai 264209, China

Short title: The magnetism tuned by charge states for SnO_2:C materials.

PACS: 75.47. Lx

Abstract: To analyze the controversial conclusions on the magnetism of C-doped SnO_2 (SnO_2:C) bulk materials between theoretical calculations and experimental observations, we propose the critical role of charge states of defects on the geometric structures and the magnetism and carry out series of first principle calculations. By changing the charge states, we can affect bader charge distributions and atomic orbital occupancies in bulk SnO_2:C systems, which conduct magnetism consequently. In all charged SnO_2:C supercells, C-2p_x/p_y/p_z electron occupancies are changed manifestly by the charge self-regulation and thus make C-2p orbitals spin polarized, which contribute the dominant magnetic moment to the system. When the concentration of C dopant in SnO_2 supercell increases, the charge redistribution assigns extra electrons averagely to each dopant and thus modulates the magnetism effectively. These findings provide an experimentally viable way for controlling magnetism in these systems.

1. Introduction

Since Dietl et al.[1] demonstrated the high Curie temperature ferromagnetism (FM) in Mn-doped GaAs, diluted magnetic semiconductors (DMSs) have been a major focus of magnetic semiconductor research.[2] Tin dioxide (SnO_2) is considered as a promising candidate of DMSs after Ogale et al. found the giant FM in Co-doped SnO_2.[3-8] The recent interest in DMSs was stimulated when magnetism emerged in materials composed of 'non-magnetic' elements that can introduce holes into valence band (VB), which is called d^0 ferromagnetism.[9-11] A good example of nonmagnetic impurity is carbon (C). It is expected that with the valence electron shell configuration of $2s^2 2p^2$, C substitution of O atoms (electron shell: $2s^2 2p^4$) forms open shell and thus conducts local magnetic moment in bulk oxides. For example, C doping can produce magnetism in alkaline-earth chalcogenides[12] and CaO.[13] Hence the magnetism of C-doped SnO_2 (SnO_2:C) has been studied both experimentally and theoretically. However, a theoretical group reported that C substitution of O (C_O defect) can only create magnetism in (001) surface of SnO_2, not in the interior of bulk SnO_2 lattice.[14] This is difficult to understand because C dopant can induce FM in ZnO and TiO_2, especially the latter has the same rutile structure as SnO_2. Nevertheless, the recent experimental measurements showed that SnO_2:C films conduct high temperature FM not only at/near the surface, but also in deeper layers and throughout the bulk.[15] Xiao et al. reported the magnetic moment contributed by C_O-V_O complex in bulk SnO_2:C.[16] They proposed that the diversity of the magnetism and electronic structure in SnO_2:C depends on the interplay between the existence of two stable tin oxides (Sn^{+4} in SnO_2 and Sn^{+2} in SnO), the localization of the 2*p* orbitals of C and O, and the oxygen vacancy (V_O). Electrons donated by V_O and compensated through Sn reduction process modulate the variety of magnetic ground state.

Therefore, it gives us an indication that the key point of the explanation in the magnetism of bulk SnO_2:C may lies in the free electrons redistribution induced intrinsically or extrinsically.[17] It is proposed that the magnetic coupling between these defect-induced moments is a result of delicate interplays between localization, defect charge states, and Jahn-Teller distortions.[18, 19] The band spin splitting produced by substitutional doping accompanied by depletion of the electron and hole density was observed in ZnO,[20], MgO,[21] etc., as well as in SnO_2 with intrinsic defects.[22, 23] However, the influence of charge states, i.e. the electrons distributions in SnO_2:C materials is not researched. Therefore, we carried out a series of first-principle calculations on this issue and found that the electrons redistribution in charged SnO_2:C system is a critical factor to analyze the observed magnetism.

2. Calculation methods

First-principle calculations based on density functional theory implemented in *Vienna Ab initio Simulation Package (VASP)*[24] have been carried out. The electron-electron exchange and correlation effects are described by GGA functional with PBE method.[25] The electronic wave functions are expanded using projector augmented wave method[26] with a cutoff kinetic energy of 480 eV. To simulate SnO_2:C bulk materials, a 2×2×2 rutile SnO_2 supercell is adopted and a C atom is substituted at O site, as shown in Figure 1. The geometry optimization is achieved by relaxing the internal position of atoms and the lattice parameters until the residual force is 0.01 eV/Å. The self-consistent convergence accuracy is set to 10^{-5} eV. A 3×3×4 Monkhorst-Pack mesh is used to integrate the first Brillouin zone.

3. Results and dicussions

It is well known that the electronic properties and the magnetic properties are determined by the geometric structures, i.e., the atomic arrangement in solid materials. We constructed the geometric structures of bulk SnO_2 with and without C dopant. In SnO_2:C supercell, C dopant is substituted at O site with number I in Figure1. All the optimized lattice parameters are listed in Table 1. Lattice parameters of SnO_2 increase after C_O doping because the radius of C atom is larger than that of O atom. However, the atomic size of an element is not a constant as one might expect, it is determined by both the intrinsic size (e.g., the covalent radius) and the electronic environment.[27, 28] Hence the dopant induced volume change arises as a result of two factors: the intrinsic size difference ΔV_i and the electronic environment induced volume change ΔV_e. So the charge state of defect is also a critical parameters to determine the geometry structure of SnO_2:C supercells. Charge state q represents electrons being added to or removed from the defective system, namely, the change for the number of electron or hole carriers, which may implies the change in oxidation state of a particular defect. The lattice parameters of SnO_2:C supercells with charge ranging in [-2,+2] are also described in table 1. It is evident that when C dopant has the positive charge state, the decrease of the total number of electrons in the supercell weakens the pressure of the electron gas. Therefore, this kind of electronic environment induces a negative global volume change, namely, the supercell shrinks. While if C dopant has the negative charge state, there are extra valence electrons in the supercell and thus the electron gas pressure increase, making the lattice expands. The common method used to change the charge state of a defect is to consider electrons exchange with another defect.[29] In O-poor conditions, V_O is a defect with low formation energy. So we examined the interaction of C_O with V_O defect in terms of the charge switching between C_O and V_O to explore its effect on the geometry structure and the magnetic properties. From data in Table 1, we can see that the change of lattice parameters for C_O-V_O containing system are similar as that of the negative charged SnO_2:C system, resulting from the fact that V_O donates two extra electrons to the supercell, just like the case in negative C_O defect. We also found that variations of the lattice parameters induced by the negative charged C_O defect (C_O^{-1}, C_O^{-2} and C_O-V_O) are larger than that induced by the positive charge states (C_O^{+1}, C_O^{+2}). It is well known that the wavefunctions of extra free electrons in lattice are more dispersed than that of holes, so the repulsion conducted by the free electron gas is much larger, resulting in a stronger lattice distortion for supercells with negative charged defect.

We calculated the formation energies of defects mentioned above to represent their relatively concentration in materials. The formation energy is an energy required for the creation of each defect in crystal. The formation energy of a defect α in charge state q is defined as[30, 31]

$$E^{for}[\alpha, q] = E_{tot}[\alpha, q] - E_{tot}[perfect] + \sum_i n_i\mu_i + q[E_F + E_V + \Delta V(\alpha, q)] \quad (1)$$

Here $E_{tot}(\alpha,q)$ is the total energy of the supercell with defect α in charge q, and $E_{tot}(perfect)$ is the total energy of the perfect SnO_2 supercell. n_i is the element i added to (n_i<0) or removed from (n_i>0) the perfect supercell to form a defective supercell. μ_i is the chemical potential of the reservoir of element i, which are calculated from O_2 molecule, diamond-like C and metal Sn materials for μ_O, μ_C and μ_{Sn}, respectively. The charge state q indicates the number of electrons taken from or added to the electron reservoir.[32, 33] E_F denotes the chemical potential of the electron reservoir, i.e., Fermi level. E_V denotes the energy level of valence band maximum (VBM) of pristine SnO_2, and $\Delta V(\alpha,q)$ is the offset between VBM of pristine SnO_2 and defective SnO_2:C supercells. The preferred method to align the electrostatic potentials by inspecting the core level in

the charged defective supercells far from the defect and aligning it with the electrostatic potential in pristine SnO_2, generating the needed $\Delta V(\alpha,q)$ in equation (1).[34-36] The calculated $E^{for}(\alpha,q)$ using equation (1) are listed in Table 1. If E_F is pinned at VBM, $E^{for}(\alpha,q)$ of C_O defect changes slightly with variation of charge states. When E_F shifts up towards conduction band minimum (CBM), $E^{for}(\alpha,q)$ of C_O^{-1} and C_O^{-2}decrease manifestly, indicating the more possibility for negative C_O defects to format.

We calculated the total and partial density of states (PDOS) of bulk SnO_2:C materials to explore the atomic origin of the magnetism. Our results show that neutral C_O does not induce any spin polarization in bulk SnO_2:C, which is consistent with previous calculations.[14, 16] To change the defect charge state, the common method is exchanging electrons with another defect. As reported previously, V_O plays an important role in the magnetic properties of pristine or doped SnO_2 materials.[2] So we examined the interaction of C_O with V_O defect in terms of the charge switching between C_O and V_O to explore its effect on the magnetic properties, where C_O and V_O locate at I and II sites, respectively, as shown in figure 1. The spin splitting can be seen from PDOS in figure 1 for SnO_2 supercell with C_O-V_O complex. It is interesting to see that V_O activates the magnetism in nonmagnetic SnO_2:C materials. V_O defect acts as donor in SnO_2 host and donates two electrons to compensate holes generated by C_O defect. However, electrons provided by V_O can also be partially compensated by the reduction of Sn^{+4} to Sn^{+2}. So we believe that these two electrons donated by V_O do not completely compensate the two holes yielded by C_O and the extra electrons distributed over C dopant and the rest host atoms. The charge redistribution induces spin splitting in C-2*p* orbitals.

As found the key role in DMSs played by the electron redistribution, we turn our attention to cases of bulk SnO_2 with C_O defect in -2, -1, +1, +2 charged states, namely, adding or removing one/two electrons to/from the neutral SnO_2:C systems. The emergence of magnetism is represented by the polarization energy E_{pol}, i.e., the energy difference between spin-polarized and nonspin-polarized SnO_2:C system with charged defect. The negative value of polarization energy means the spin-polarized state of this system is stable than the nonspin-polarized. As listed in Table 2, all the four charged configurations favor spin polarized states, e.g. the polarization energy of C_O^{-2} equals to -0.310 eV. In these four charged configurations, the magnetic moments dominantly come from C dopants, with little contribution from the nearest neighboring (NN) Sn and the next nearest neighboring (NNN) O atoms.

Like the case in C_O-V_O system, the two injected extra electrons in C_O^{-2} defective system could compensate holes generated by the neutral C_O defect. However, the bader charge analysis shows that only 0.3 *e* could be captured by C_O defect, the rest are dispersed over the NN Sn atoms and other host atoms. As Sn ion is a divalent ion, i.e., Sn^{+4} and Sn^{+2}, it can accommodate excess electrons by a reduction reaction of Sn^{+4} to Sn^{+2}. As reported previously, oxidation state does not reflect the local charge on the ion, but rather the occupancy of the respective crystal field levels.[37] The charge regulation can be illustrated clearly by the charge density difference with the variation in electron density spatial redistributions between the neutral and the charged C_O containing configurations, which is shown in figure 2. In the contour map of the charge density difference for C_O^{-2}, the most manifest change of charge density emerges in the space around C dopant. The charge density increases and decreases in the plane perpendicular to C-Sn bond ((110) plane) and in the direction along with C-Sn bond, respectively. Owing to the negative feedback,[38] the charge around C dopant changes moderately resulting from the deleting and adding of electron

occupancies in different bonding directions. The increase of electron density perpendicular to (110) plane indicates the increasing occupancies in C-2p_x/2p_y orbitals, which agrees well with the PDOS in figure 3(a) and (b).

The charge redistribution of injected electrons results in obvious change in PDOS between the neutral and the negative charged SnO_2:C systems. Comparing with neutral C_O defect, C-2p_z orbital in C_O^{-2} system (figure 3) remains the nearly full occupied state, while C-2p_x/2p_y change to be partially occupied by excess electrons captured by C dopant, leading to the spin polarization in SnO_2:C crystal with a total magnetic moment of 0.487μ_B. The coupling interactions between C, NN Sn and NNN O are conducted by hybridizations between C-2*p*, Sn-4*d* and O-2*p* wavefunctions, which are described as *p*-*d*/*p*-*p* couple.[39, 40] As listed in Table 2, the spin directions of NN Sn atom and NNN O atoms align antiparallel and parallel with that of C atoms, respectively. In real materials the direct exchange is driven by minimizing the potential energy due to reduced overlap of electron wavefunctions. The distance between C and NN Sn is near enough to give birth to a large electronic orbital overlap. The electrons spend most of the time in space between these atoms and give rise to the antiferromagnetic order due to the Pauli's exclusion principle. While NNN O atoms is a little far from C dopant, the electrons spend most of the time away from each other and give rise to the ferromagnetic order, so the spins between them are arranged in parallel directions.

It is interesting to see that the magnetic properties including polarization energies and magnetic moment distributions behave nearly in the same way for the case in C_O^{-1}, C_O^{-2} and C_O-V_O containing SnO_2 crystals. Because of the strong delocalization of the extra free electron in the lattice, when they are increased from one to two, namely, C_O^{-1} changes to C_O^{-2}, the electron density localizing around C dopant changes little. Therefore, the bader charge and thus the magnetic properties exhibit the same character for these three cases, which can be verified by PDOS and the charge density difference illustrated in figure 2 and figure 3. The charge density differences of supercell containing C_O^{-2} and C_O-V_O defects show nearly identical performances, except that the charge localization of C_O-V_O systems is stronger than the case in C_O^{-2} system. For the large lattice distortion and broken bond around defect V_O, the electrons exhibit a little more localized delocalization.

When we turn attention to the positive charged SnO_2:C materials, we also found magnetism emerges, e.g., the total magnetic moment of C_O^{+2} defective system is 1.465μ_B. The magnetism is caused by the two holes induced in +2 charged SnO_2:C supercell. These holes make C-2*p* and NNN O-2*p* orbitals unoccupied and then form d^0 magnetism, which can be proved by PDOS of C_O^{+2} containing system, as plotted in figure 3(c) and (d). Comparing with the negative charged states, E_F in positive charged SnO_2:C system shifts downward into VB, with only small portion of majority spin C-2p_x/p_y/p_z being occupied, the variation of electron occupancies in C-2*p* orbital conducts spin splitting in PDOS of this orbital. The most obvious change is that the minority spin C-2p_z orbital shifts up above E_F and becomes unoccupied. The O-2*p* orbital also shows large spin splitting and contributes unnegligible magnetic moment to the total system. When C_O defects is in negative charged state, the host O-2*p* orbital is full occupied and nearly could not be affected by the injected extra electrons, so O-2*p* orbital shows small contribution to the total magnetic moment. However, when SnO_2:C system is positive charged, the enforcement of O-2*p* spin splitting originates from the fact that holes are induced into host crystals. From the electron density difference in figure 2(b), we noted that holes do not only distribute around C dopant, but

also distribute in the space around NNN O atoms. The charge redistribution makes the electron occupancy of NNN O-2*p* orbital change and then conducts a larger magnetic moment than ever. Our conclusions agree well with the previous reports that the electron deletion effect contributes to greater splitting of the conduction and valence bands in crystal structure.[41]

Considering the dopant concentration effect, two O impurity are substituted by two C atoms in SnO_2 lattice, and then things become interesting and more complicated. We employ five configuarations to simulate the carbon impurity distributions in the supercell. As illustrated in Figure 1, two C dopants locate at position (III, IV), (III, V), (III, VI), (VII, VIII) and (VII, IX), respectively, which are signaled as Cf.1, Cf.2, Cf.3, Cf.4 and Cf.5, respectively. The calculated results for these five configurations in neutral charge state are listed in Table 3. For neutral charged SnO_2 supercell, when the distance between two substitutional C dopants is near, i.e., both C dopants substitute the NNN O positions, for instance, Cf.1 and Cf.2, magnetism emerges, as reported previously.[16] In each of these two configurations, two C atoms contribute to the total magnetic moment equavilently. However, when the distance between two C dopants increases, magnetism disappears. This means that the atomic orbital hybridization between two C dopants via space overlap provides the predominant contribution to the magnetism. However, space overlap between orbital wavefuncitons decreases with the increase of distance between two C dopants in SnO_2 supercell and turns the magnetism to null eventually. This short-range magnetism can not account for the experimentally observed collective magnetism. So we also adopt the strategy of adjusting the valence electons/charge state to study the magnetism induced by charge redistribution in a couple of C impuritys doped SnO_2 system.We take Cf.1 and Cf.4 for example, i.e., one configuration with NNN C dopant pair and another with C dopant pair far away from each other. Magnetism emerges in both configurations when two excess electrons are added. For Cf.1, i.e., the configuration being spin-polarized original, the magneism is weakened by the electron injection. Two extra electrons do not localize at one specific atoms, but distribut over the full space of supercell, predominantly around the space near the couple of C_O defects. As illustrated in Figure 4(a), the electrons captured by two C_O defects are equivalent. The captured electrons change the occupancies of C-2*p*/O-2*p*/Sn-4*d* orbitals and partially compensate the holes in these orbitals contributing to the total magnetic moment. Thus the spin-polarizations of these orbitals are weakened and the polarization energy and total magnetic moment decrease. On the other hand, Cf.4 changes to be magnetic when two extra electrons are introduced, which is nonmagnetic originally. The electrons and magnetic moment localize around each C dopant are 5.054 *e* and 0.426 μ_B, just like the case in C_O^{-1} defective system mentioned above. This can be seen more clearly from the charge difference map plotted in Figure 4(b), in which the charge redistribution around each C dopant is similar as the one of C_O^{-1} in Figure 2(a). For Cf.4, two C dopants are too far to yield effective interactions between each other, so it looks like the simple superimposing of two isolated C dopant in one supercell. When two extra electrons moves in, they are nominally shared averagely by two C dopant, making the magnetism of Cf.4 with -2 charge state to be superimposing of two single C_O^{-1} defect containing system.

As discussed above, the magnetism originates from the charge redistribution in all mentioned SnO_2:C bulk materials with various charge states. The dominant contribution of magnetic moment comes from C-2*p* orbitals, which should be quite localized. However, considering the unclear reperesentation of electron exchange-correlation potential, the localization of C-2*p* orbitals may not be depicted reasonablly by GGA method of density functional theory. Hence, we carried out

series of hybrid functional (HSE06 function)[42] calculations to check if GGA method give rational results for the magnetism of SnO_2:C materials. By inspection of the HSE calculation results, we find that except the more accurrate value of band gaps, the influence brought by HSE function on the localized spin-polarization of atomic orbitals is inconspicuous. For example, we illustrate PDOS of SnO_2:C materials in neutral and -2 charge state in Fig.S1 in the supplementary materials, which is calculated by HSE06 functions. PDOS of neutral charged SnO_2:C calculated by GGA method is also plotted in Fig.S2 in supplementary materials for comparison. The HSE calculated PDOS shows manifest localized spin-polarized states in both C-2*p* and Sn-5*s* orbitals, just like the data obtained from GGA calculations. The total magnetic moment and magnetic moment projecting on C dopant in -2 charged system are 0.478 μ_B and 0.443 μ_B, respectively, that is, the nearly equivalent value of GGA calculations. So the localization of atomic orbitals is not sensitive to the hybrid functional calculations and thus analyses based on GGA results just mentioned above are sufficient.

4. conclusions

By performing series of first principle calculations, we found that the magnetism in bulk SnO_2:C materials can be tuned via changing charge states of C_O defect. The critical role on the geometric structure and thus the magnetism of SnO_2:C systems played by charge self-regulation is confirmed. The induced free electrons or holes change the bader charge and the magnetic moment distributions in charged SnO_2:C materials. In all charged SnO_2:C supercells, the dominant contributions of magnetic moments come from C-2*p* orbitals, which are caused by the variation of electron occupancies in C-2$p_x/p_y/p_z$ orbitals. When there are two C being doped into SnO_2 lattice, the charge redistribution assigns the extra electrons averagely to each dopant and thus modulate the magnetism effectively. These findings may provide rational explanation for the magnetism observed in bulk SnO_2:C materials and suggest an experimentally viable way for controlling magnetism in these systems.

Achnowledgments

This work is supported by the National Science foundation of China under Grant U1231103 and 41473065, and the Science Foundation for Youth of Shandong University at Weihai.

References

1 **T. Dietl, H. Ohno, F. Matsukura, J. Cibert, and D. Ferrand, Science, 2000, 287, 1019-1022.**

2 **G. S. Chang, J. Forrest, E. Z. Kurmaev, A. N. Morozovska, M. D. Glinchuk, J. A. McLeod, A. Moewes, T. P. Surkova, and N. H. Hong, Phys. Rev. B, 2012, 85, 165319.**

3 **B. Zhou, P. Wu, and W. Zhou, Appl. Phys. Lett. , 2012, 101, 182406.**

4 **H. Nguyen Hoa, R. Antoine, W. Prellier, S. Joe, and H. Ngo Thu, J. Phys.: Condens. Matter 2005, 17, 6533.**

5 **H. Nguyen Hoa, S. Joe, W. Prellier, and H. Awatef, J. Phys.: Condens. Matter 2005, 17, 1697.**

6 **W. Cen, Q. Wu, H. L. Ge, S. Tao, and J. Z. Jiang, Nanotechnology, 2012, 23, 075704.**

7 **G. M. Stoian, P. A. Stampe, R. J. Kennedy, Y. Xin, E. Lochner, and S. v. Molnár, J. Phys. D: Appl. Phys. , 2014, 47, 295002.**

8 R. Djulgerova, L. Popova, G. Beshkov, Z. L. Petrovic, Z. Rakocevic, V. Mihailov, V. Gencheva, and T. Dohnalik, J. Phys. D: Appl. Phys. , 2006, 39, 3267.

9 K. S. Yang, Y. Dai, B. B. Huang, and Y. P. Feng, Phys. Rev. B, 2010, 81, 033202.

10 M. Venkatesan, C. B. Fitzgerald, and J. M. D. Coey, Nature, 2004, 430, 630.

11 K. S. Yang, R. Q. Wu, L. Shen, Y. P. Feng, Y. Dai, and B. B. Huang, Phys. Rev. B, 2010, 81, 125211.

12 J. Liu, L. Chen, H.-N. Dong, and R.-L. Zheng, Appl. Phys. Lett. , 2009, 95, 132502.

13 V. Pardo and W. E. Pickett, Phys. Rev. B, 2008, 78, 134427.

14 G. Rahman and V. c. M. García-Suárez, Appl. Phys. Lett. , 2010, 96, 052508.

15 N. Hoa Hong, J. H. Song, A. T. Raghavender, T. Asaeda, and M. Kurisu, Appl. Phys. Lett. , 2011, 99, 052505.

16 W.-Z. Xiao, L.-L. Wang, and Z. Tan, Comput. Mater. Sci. , 2014, 83, 5-11.

17 F. Ming, T. Xiaoli, C. Xueli, Z. Lide, L. Peisheng, and J. Zhi, J. Phys. D: Appl. Phys. , 2007, 40, 7648.

18 A. Stroppa, G. Kresse, and A. Continenza, Phys. Rev. B, 2011, 83, 085201.

19 P. Ruiz-Díaz and V. S. Stepanyuk, J. Phys. D: Appl. Phys. , 2014, 47, 105006.

20 P. Dev and P. Zhang, Phys. Rev. B, 2010, 81, 085207.

21 H. K. Chandra and P. Mahadevan, Phys. Rev. B, 2014, 89, 144412.

22 W. Wei, Y. Dai, M. Guo, K. R. Lai, and B. B. Huang, J. Appl. Phys. , 2010, 108, 093901.

23 S. Ghosh, G. G. Khan, and K. Mandal, ACS Appl Mater Interfaces, 2012, 4, 2048-2056.

24 G. Kresse and J. Furthmüller, Phys. Rev. B, 1996, 54, 11169-11186.

25 G. Kresse and D. Joubert, Phys. Rev. B, 1999, 59, 1758-1775.

26 P. E. Blochl, Phys. Rev. B, 1994, 50, 17953-17979.

27 J. Zhu, F. Liu, G. B. Stringfellow, and S.-H. Wei, Phys. Rev. Lett. , 2010, 105, 195503.

28 Y.-B. Lu, Y. Dai, W. Wei, Y. T. Zhu, and B. B. Huang, ChemPhysChem, 2013, 14, 3916-3924.

29 A. Punnoose, K. Dodge, J. J. Beltrán, K. M. Reddy, N. Franco, J. Chess, J. Eixenberger, and C. A. Barrero, J. Appl. Phys. , 2014, 115, 17B534.

30 S.-H. Wei and S. Zhang, Phys. Rev. B, 2002, 66, 155211.

31 L. Torpo, M. Marlo, T. E. M. Staad, and R. M. Nieminen, J. Phys.: Condens. Matter 2001, 13, 6203-6231.

32 N. Cowern, K. Janssen, G. van de Walle, and D. Gravesteijn, Phys. Rev. Lett. , 1990, 65, 2434-2437.

33 I. O. Usov, A. A. Suvorova, V. V. Sokolov, Y. A. Kudryavtsev, and A. V. Suvorov, J. Appl. Phys. , 1999, 86, 6039.

34 C. G. Van de Walle and J. Neugebauer, J. Appl. Phys. , 2004, 95, 3851-3879.

35 Y.-H. Li, A. Walsh, S. Chen, W.-J. Yin, J.-H. Yang, J. Li, J. L. F. Da Silva, X. G. Gong, and S.-H. Wei, Appl. Phys. Lett. , 2009, 94, 212109.

36 A. Klein, J. Am. Ceram. Soc. , 2013, 96, 331-345.

37 P. A. Stolk, et al., J. Appl. Phys. , 1997, 81, 6031-6050.

38 H. Raebiger, S. Lany, and A. Zunger, Nature, 2008, 453, 763-766.

39 Y.-B. Lu, Y. Dai, M. Guo, L. Yu, and B. B. Huang, Phys. Chem. Chem. Phys. , 2013, 15, 5208-5214.

40 L. Liu, P. Yu, Z. Ma, and S. Mao, Phys. Rev. Lett. , 2008, 100, 127203.

[41] J. Berashevich and A. Reznik, J. Phys. Chem. Solids 2014, 75, 1132-1136.
[42] J. Heyd, G. E. Scuseria, and M. Ernzerhof, J. Chem. Phys., 2006, 124, 219906.

Table 1. The lattice parameters and the formation energy (E^{for}) under Sn-rich condition for SnO_2:C materials in various charge states. The lattice parameters and the energies are represented in units of Å and eV, respectively. E_f is Fermi level.

defect	E^{for}	a	c
pure		4.822	3.243
C_O^{-2}	6.384-2E_f	4.943	3.286
C_O^{-1}	4.399-E_f	4.886	3.264
C_O^{0}	4.848	4.845	3.253
C_O^{+1}	4.981+E_f	4.808	3.241
C_O^{+2}	5.515+2E_f	4.77	3.235
V_O-C_O	5.423	4.873	3.252
TiO_2:C	5.702	4.682	2.970

Table 2. The polarization energy E_{pol}, i.e., the energy difference between spin-polarized and nonspin-polarized SnO_2:C system with charged defect. μ_T, μ_C, μ_{Sn} and μ_O denote the total magnetic moment (μ_B/supercells) and the magnetic moment contributed by C dopant, NN Sn atoms and NNN O atoms, respectively. The bader charge distributions on C dopant, NN Sn atoms and NNN O atoms are denoted as Q_C, Q_{Sn} and Q_O, respectively. The corresponding values for C substitution O plus one O vacancy(C_O-V_O complex) are also listed here.

q	$E_{pol}(eV)$	$\mu_T(\mu_B)$	$\mu_C(\mu_B)$	$\mu_{Sn}(\mu_B)$	$\mu_O(\mu_B)$	$Q_C(e)$	$Q_{Sn}(e)$	$Q_O(e)$
-2	-0.310	0.487	0.423	-0.013	0.061	5.069	11.815	7.217
-1	-0.324	0.508	0.423	-0.013	0.069	5.072	11.771	7.217
0	0	0	0	0	0	4.791	11.716	7.208
+1	-0.094	0.695	0.330	0.061	0.247	4.616	11.650	7.204
+2	-0.141	1.465	0.582	0.094	0.480	4.497	11.648	7.192
V_O-C_O	-0.338	0.537	0.446	-0.009	0.079	4.950	11.762	7.172

Table 3. The distance (L) between two dopants in SnO_2 lattice, the polarization energy E_{pol}, i.e., the energy difference between spin-polarized and nonspin-polarized SnO_2:C system with charged defect. μ_T, μ_{Sn} and μ_O denote the total magnetic moment and the magnetic moment contributed by C dopant, NN Sn atoms and NNN O atoms, respectively. μ_{C1} and μ_{C2} denotes the magnetic moments contributed by the two C dopant separately.

	q	L(Å)	E_{pol}(eV)	$\mu_T(\mu_B)$	$\mu_{C1}(\mu_B)$	$\mu_{C2}(\mu_B)$	$\mu_{Sn}(\mu_B)$	$\mu_O(\mu_B)$
Cf.1	0	2.639	-0.334	2.493	0.802	0.802	0.22	0.595
	-2	2.912	-0.236	1.038	0.456	0.456	-0.012	0.138
Cf.2	0	3.243	-0.278	1.080	0.454	0.454	0.454	0.109
Cf.3	0	4.180	0.000	--	--	--	--	--
Cf.4	0	4.822	0.000	--	--	--	--	--
	-2	4.947	-0.697	1.016	0.426	0.426	-0.010	0.166
Cf.5	0	6.819	0.000	--	--	--	--	--

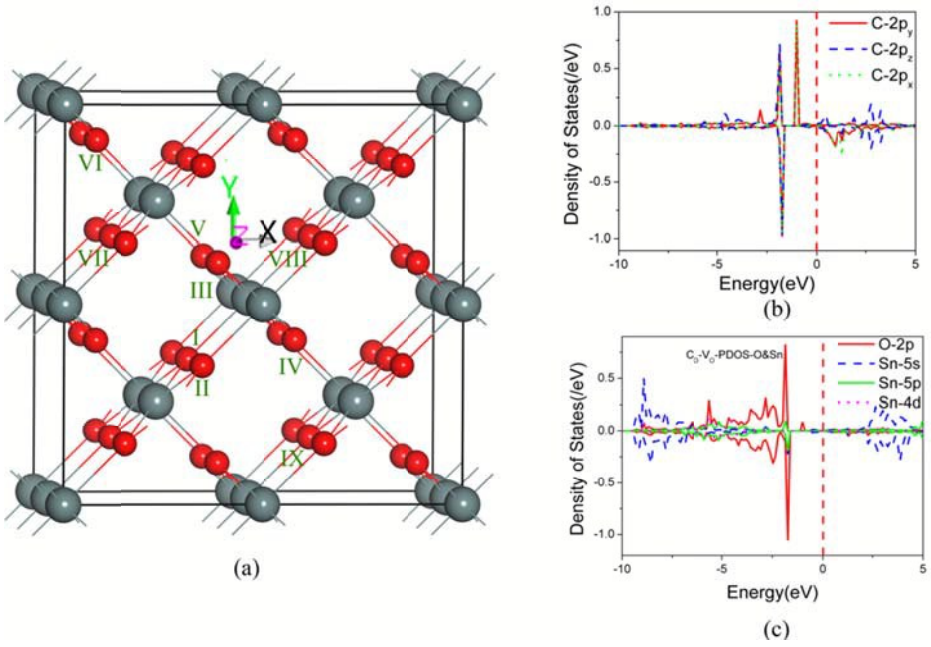

Figure1. (a) The geometry structures of bulk SnO_2 materials and the PDOS projected on (b) C dopant and (c) Sn, O atoms in SnO_2 supercell with C_O-V_O complex, respectively. The gray and red balls in (a) denote Sn and O atoms, respectively. The Roman numerals in (a) represent the location of C_O and V_O defects in SnO_2:C crystal, respectively. The vertical red dashed line in (b) and (c) represents Fermi level.

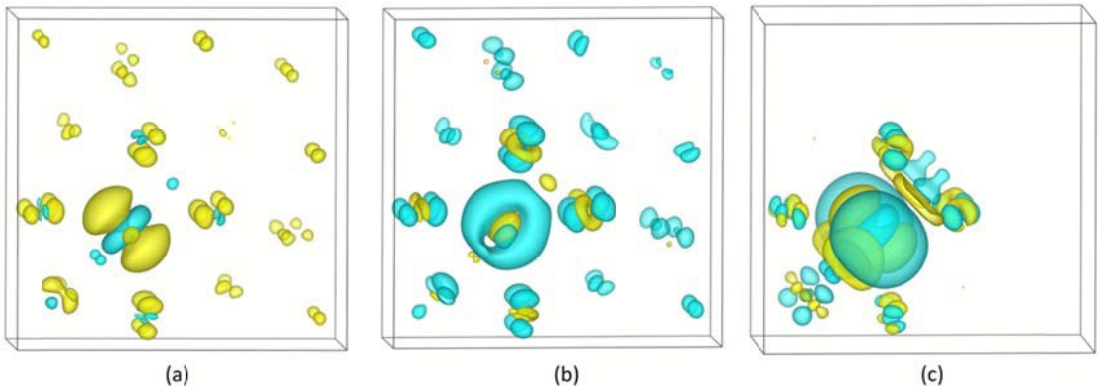

Figure 2. Charge density differences between (a) -2 charged and neutral SnO_2:C; (b) +2 charged and neutral SnO_2:C ; (c) C_O-V_O complex and neutral SnO_2:C, respectively. The yellow and blue isosurfaces represent increase and decrease in the total charge density, respectively.

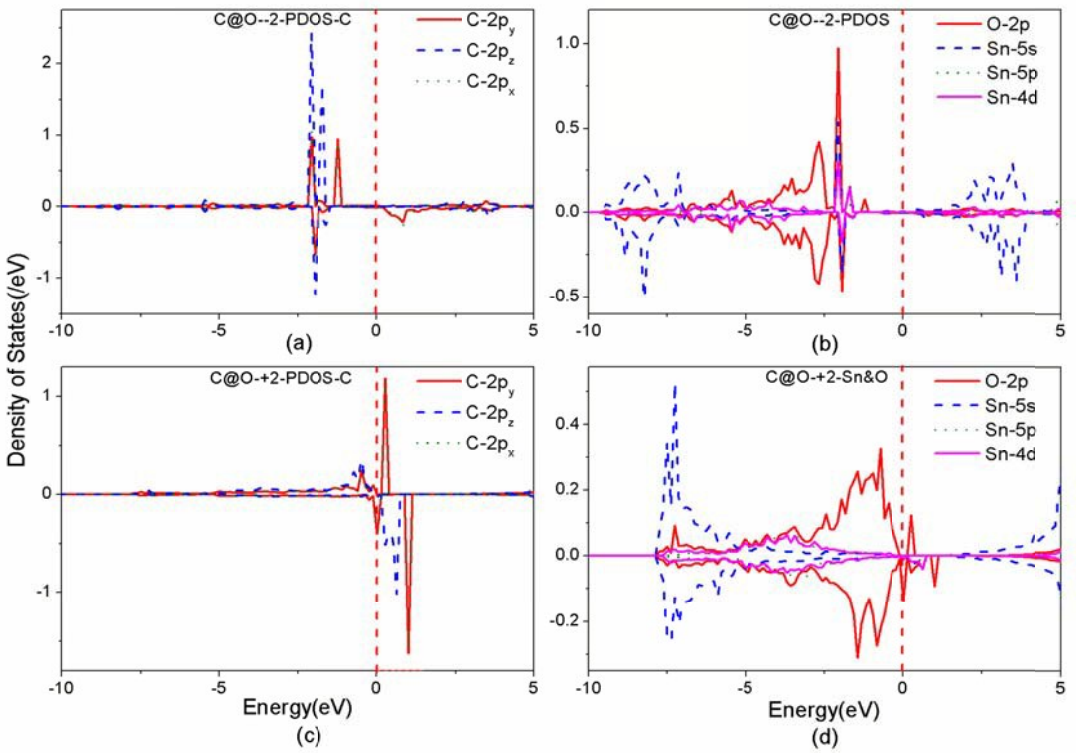

Figure 3. PDOS of C_O defects in charged states. (a) and (b) demonstrate PDOS of C dopant and NN-Sn/NNN-O atoms in C_O^{-2} states, respectively. (c) and (d) demonstrate PDOS of C dopant and NN-Sn/NNN-O atoms in C_O^{+2} states, respectively. The vertical red dashed line represents Fermi level.

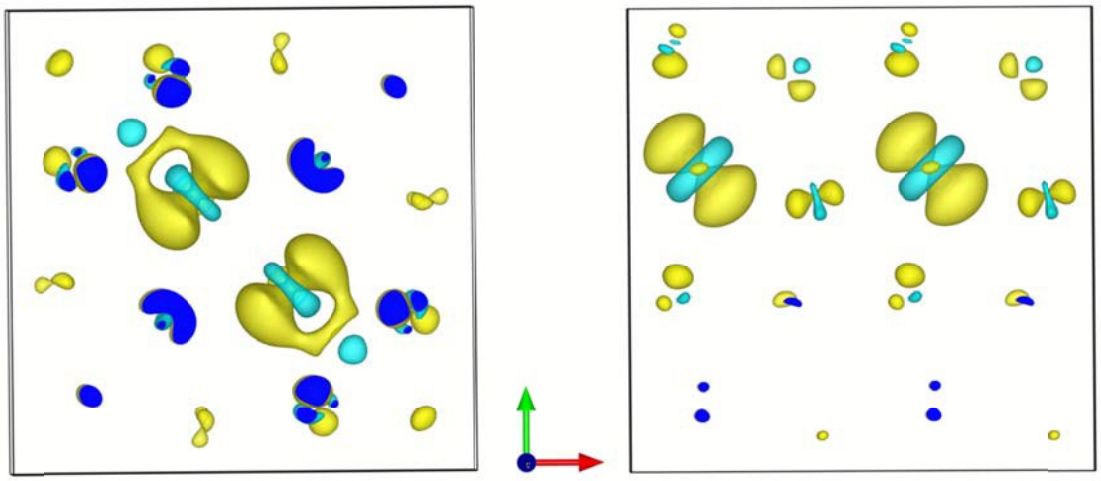

Figure 4. Charge density differences between -2 charged and neutral 2C doped SnO_2 materials for (a) Cf.1 and (b) Cf.4, respectively. The yellow and blue isosurfaces represent increase and decrease in the total charge density, respectively.